MedCrave
Step into the World of Research
Journal of Analytical & Pharmaceutical Research

Research Article

Open Access
CrossMark

# Inhibition potential of the major secondary metabolites isolated from *anacardium occidentale* against Mpro enzyme from COVID-19 virus using molecular docking and dynamics studies

## Abstract

The sanitary emergency installed in the world generated by the pandemic COVID-19 instigates the search for scientific strategies to mitigate the damage caused by the disease to different sectors of society. The disease caused by the coronavirus, SARS-CoV-2, reached 216 countries/territories, where about 20 million people were reported with the infection, and more than 740,.000 died. Given the situation, research involving the development and validation of new antiviral molecules, especially against the SARS-CoV-2 virus, is highly relevant. In this work, a *in silico* study was carried out to evaluate the inhibitory power of phytoconstituents from *Anacardium occidentale L.* against Mpro enzyme from COVID-19 virus. The molecular docking simulations were performed to understand interactions between some phytochemicals present in *A. occidentale* against the Mpro enzyme from SARS-CoV-2, the amentoflavone and agathisflavone molecules showed the best affinity energy in the value of -8.0 kcal/mol and -8.3 kcal/mol, respectively. The molecular dynamics results indicated that the agathisflavone ligand had interactions more stable and a highest interaction potential energy with the Mpro enzyme than the amentoflavone ligand.

**Graphical abstracts**

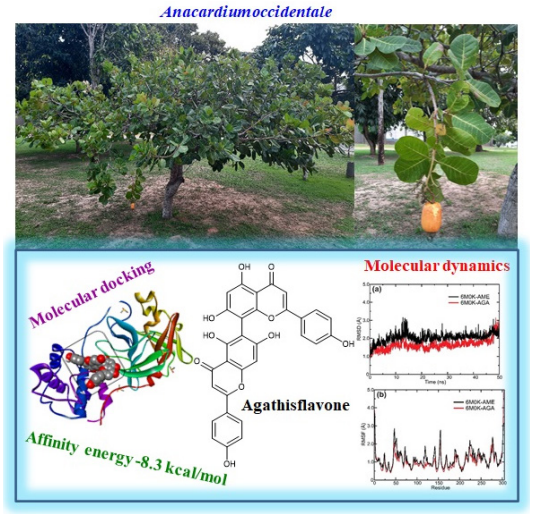


**Keywords:** *anacardium occidentale*, molecular docking, molecular dynamics, SARS-CoV-2

Volume 11 Issue 2 - 2022

Antônio MG Pereira,[1] Lucas L Bezerra,[2] Márcia M Marinho,[3] Emanuel Paula Magalhaes,[4] Ramon RPPB de Menezes,[4] Tiago L Sampaio,[4] Paulo N Bandeira,[2] Carla FC Fernandes,[5] Emmanuel S Marinho,[6] Alexandre MR Teixeira,[1] Hélcio S dos Santos[1,2,7]

[1]Programa de Pós-Graduação em Biotecnologia - PPGB-Renorbio, Universidade Estadual do Ceará, Fortaleza, CE, Brasil
[2]Universidade Estadual do Vale do Acaraú, Centro de Ciências Exatas e Tecnologia, Sobral, CE, Brasil
[3]Faculdade de Educação, Ciência e Letras de Iguatu, Universidade Estadual do Ceará, Iguatu, Ceará, Brasil
[4]Universidade Federal do Ceará, Departamento de Análises Clínicas e Toxicológicas, Fortaleza, CE, Brasil
[5]Universidade Estadual do Ceará, Faculdade de Filosofia Dom Aureliano Matos, Limoeiro do Norte, CE, Brasil
[6]Fundação Oswaldo Cruz, Laboratório Multiusuário de Pesquisa e Desenvolvimento - Plataforma de Anticorpos e Nanocorpos, Eusébio, CE, Brasil
[7]Universidade Estadual do Ceará, Centro de Ciências e Tecnologia, Programa de Pós-Graduação Ciências Naturais, Fortaleza, Ceará, Brasil

**Correspondence:** Hélcio S dos Santos, Universidade Estadual do Ceará, Centro de Ciências e Tecnologia, Programa de Pós-Graduação Ciências Naturais, Fortaleza, Ceará, Brasil, Email helcio.silva@uece.br

**Received:** February 18, 2022 | **Published:** March 08, 2022

## Introduction

The first reports related to covid (CoV) with severe respiratory syndromes, emerged in China in the early 2000s, posteriorly, in 2002 and 2003, more than 8 thousand cases of the disease and 774 deaths were mentioned, concentrated in eastern and western Asia, as well as reports of deaths in South Africa, Central America and Europe.[1] Recently, a new coronavirus was discovered, named SARS-CoV-2, which may cause severe acute respiratory disease in humans.[2] This respiratory syndrome formerly known as new coronavirus 2019 (2019-nCoV), is a respiratory disease resulting from infection caused by the new coronavirus, which has enveloped RNAs widely distributed among humans, other mammals, and birds and that cause respiratory, enteric, hepatic, and neurological diseases.[3] Besides, the COVID-19 spreads primarily through the respiratory tract, by droplets, respiratory secretions, and contact.[4]

No specific drug has been approved for coronavirus 2019 disease (COVID-19) to date, as the development of antivirals often takes time. Therefore, evaluation and using of currently available antiviral drugs are essential for a timely response to the current pandemic. In this context, we may highlight the plant species *Anacardium occidentale* L., popularly known as cashew tree (Figure 1), native to Brazil, found abundantly in the biodiversity of the Northeast, where it stands out

for its high socioeconomic importance for the region, representing 99.7% of the Brazilian exports of cashew nuts (the main product of the cashew crop).[5] Phytochemical studies report the isolation of several constituents, mainly phenolic compounds (Figure 2). Additionally, this species presents several pharmacological properties such as antimicrobial activity,[6] antifungal antioxidant,[7] larvicide and antiacetylcholinesterase[8] and antidiabetic activity.[9] In this work, the inhibition potential of the major secondary metabolites isolated from *A. occidentale* against Mpro enzyme from COVID-19 virus were evaluate using molecular docking and dynamics studies.

**Figure 1** *Anacardium occidentale* species.

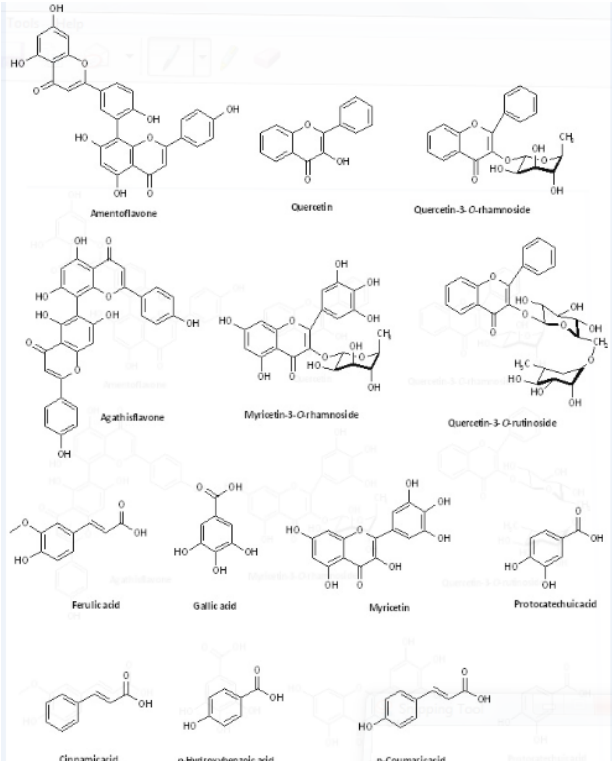


**Figure 2** Structural representation of the main isolated constituents from the *Anacardium occidentale*.

# Materials and methods

## Obtaining the structures

To perform this work, the Pubchem® online molecular repository (http https://pubchem.ncbi.nlm.nih.gov/) was used to obtain the two-dimensional coordinates of the ligands (Agathisflavone (PubChem CID: 5281599), Amentoflavone (PubChem CID: 5281600), quercetin-3-*O*-rhamnoside (PubChem CID: 5280459), Myricetin (PubChem CID: 5281672), myricetrin-3-*O*-rhamnoside (PubChem CID: 5281673), gallic acid (PubChem CID: 370), cinnamic acid (PubChem CID: 444539), *p*-coumaric acid (PubChem CID: 637542), ferulic acid (PubChem CID: 445858), protocatechuic acid (PubChem CID: 72), p-hydroxybenzoic acid (PubChem CID: 135), quercetin 3-*O*-rutinoside (PubChem CID: 5280805), and Quercetin (PubChem CID: 5280343)), then plotted in the .mol format in the MarvinSketch© *software* (https://chemaxon.com/products/marvin).[10]

## Structural optimization

For structural optimization, the semi-empirical quantum formalism was used[11] through algorithms available in the Molecular Orbital Package code (MOPAC) 2016, Version 16.111W, being used for the optimization method. The Parametric Method 7 (PM7),[12] with the Hartree-Fock approximation (HF) (self-consistent field method), for wave function.[13] The simulations were configured to perform continuous calculations of cycles of 500 interactions with a convergence value in the order of $10^{-10}$ kcal.mol$^{-1}$. In this stage, the conformational stability of the compound is given by the total energy, which is the sum of the nuclear repulsive energies with the electronic energy, obtained by solving the[12,14] All calculations performed were considering the molecule in the ground state and in a vacuum.

## Molecular docking

The structure of the main protease of the COVID-19 virus ($M_{pro}$) was obtained in the PDB database, deposited under the code PDB 6M0K, identified as "The crystal structure of COVID-19 main protease in complex with an inhibitor 11b". As a comparison criterion, it was used the Baricitinib (PubChem CID:44205240), Remdesivir (PubChem CID:121304016), Azithromycin (PubChem CID:447043), and Anakinra drugs (PubChem CID: 139595263) selected in the PubChem repository (https://pubchem.ncbi.nlm.nih.gov/). In preparing enzymatic targets, all residues were removed, and polar hydrogens were added, producing favorable protonation states for molecular docking simulations.[15]

The molecular docking simulations of the phytochemicals with the COVID-19 were subjected to a hundred independent simulations with cycles of 10 poses each. All simulations were performed using the Lamarckian Genetic Algorithm (LGA) algorithms, implemented in the AutoDock Vina code.[16] All simulations were performed with 3-way multithreading and the respective grid box parameters: center_x = -17.744, center_y = 11.691, center_z = 55.282, size_x = 110, size_y = 124, size_z = 116, spacing = 0.575, and exhaustiveness = 8.

The output files (.outligand) generated were rendered in the UCSF Chimera® *software*,[17] where the analysis of interaction and distance of the ligands was made in comparison with the catalytic sites occupied by the control ligand FJC ({N}-[(2~{S})-3-(3-fluorophenyl)-1-oxidanylidene-1-[[(2~{S})-1-oxidanylidene-3-[(3~{S})-2-oxidanylidenepyrrolidin-3-yl]propan-2-yl]amino]propan-2-yl]-1~{H}-indole-2-carboxamide). The control ligand was purchased from the original docking deposited at the Protein Data Bank (PDB).

The docking results were clustered into groups with RMSD (Root Mean Square Deviation) less than 2.0 Å.[18] To ensure the docking validity, a redocking procedure was conducted using the same parameters for the native ligands from PDB structure.[20] The data obtained from the analysis were plotted on the Morpheus® online statistical tool (https://software.broadinstitute.org/morpheus/), where heat maps were generated to identify the ligand-residue interaction profiles (L-R's) and similarity by Pearson's statistical test. The types of L-R's interactions and the Figures were generated using Discovery Studio Visualizer® *software*.[21]

### Molecular dynamics

The computational simulations with molecular dynamics (MD) were performed through GROMACS (GROningen MAchine for Chemical Simulation) 2020.4 package *software*[22] implemented with the AMBER ff99SB[23] force field. First, the best-docked pose of each ligand in the protein was utilized as a starting point for MD simulations. The parameters of Amentoflavone (AME) and Agathisflavone (AGA) molecules were obtained by script ACPYPE (AnteChamber Python Parser InterfacE).[24] Subsequently, the solvation system was realized using water molecules described by the TIP3P (Transferable Intramolecular Potential with 3 Points) model,[25] and then the system was neutralized with the additional four $Na^+$ ions. The geometry of the system was realized by the *steepest descent*[26] algorithm with $10^5$ steps and an energy tolerance at the value of 10 kJ $mol^{-1}$ $nm^{-1}$. Then, each system was equilibrated with 1 ns by ensemble NVT (constant number of particles, volume, and temperature) through of V-rescale thermostat[28] at the temperature of 310 K, followed by 1 ns ensemble NPT (constant number of particles, pressure, and temperature) by Parrinello-Rahman[29] barostat with a pressure of 1 bar. Finally, the production MD step was performed in 50 ns through Leap-Frog integrator[30] with the same temperature and pressure utilized in the equilibrium step. The VMD (Visual Molecular Dynamics)[31] *software* was used to analyze the results obtained by molecular dynamics.

## Results and discussion

### Molecular docking

The molecular docking simulations were performed to understand interactions between some phytochemicals present in *Anacardium occidentale* against the Mpro enzyme from SARS-CoV-2. Table 1 shows values of affinity energy and the Root Means Square Deviation (RMSD). The remdesivir (REM), anakinra (ANA), amentoflavone (AME), agathisflavone (AGA), ferulic acid (FER), myricetin (MYR), myricetin-3-*O*-rhamnoside (MOR), quercetin (QUE), quercetin-3-*O*-rhamnoside (QORh), quercetin-3-*O*-rutinoside (QORu), azithromycin (AZI), baricitinib (BAR), gallic acid (GAA), *p*-coumaric acid (PCA), protocatechuic acid (PRA), cinnamic acid (CIA), and p-Hydroxybenzoic acid (PHB) ligands showed values affinity energy of -6.8 kcal/mol, -6.5 kcal/mol, -8.0 kcal/mol, -8.3 kcal/mol, -4.6 kcal/mol, -6.7 kcal/mol, -7.6 kcal/mol, -6.7 kcal/mol, -7.1 kcal/mol, -7.4 kcal/mol, -5.8 kcal/mol, -5.7 kcal/mol, -5.0 kcal/mol, and -4.5 kcal/mol, respectively. All selected poses have RMSD values around 2.000 Å. Therefore, the remdesivir, anakinra, myricetin, myricetin-3-*O*-rhamnoside, quercetin, quercetin-3-*O*-rhamnoside, and quercetin-3-*O*-rutinoside ligands have a good affinity with the Mpro enzyme, due that these molecules had values affinity lower than -6.0 kcal/mol that is the considered standard in the literature.[32] In addition, the amentoflavone and agathisflavone molecules showed the best affinity energy in the value of -8.0 kcal/mol and -8.3 kcal/mol, respectively. For this reason, the molecular dynamics simulations were performed only for these ligands.

Although the anakinra ligand exhibited a value of RMSD > 2.0 Å, the high affinity indicated interactions stable and probable to occur in biological organisms.[18,33] Then, our phytochemicals would be able to interact or inhibit this target stronger, as presented previously.[34] The phytochemicals interacted in three sites of interactions in the Mpro enzyme (Figure 3a–c). In the first interaction site, the gallic acid, p-coumaric acid, and protocatechuic acid were localized in the same site that the baricitinib molecule and remdesivir inhibitor (Figure 3a). Figure 3b showed the amentoflavone, quercetin-3-*O*-rutinoside, agathisflavone, quercetin, quercetin-3-*O*-rhamnoside, myricetin, ferulic acid, and myricetin-3-*O*-rhamnoside molecules are localized in the same site that the reference drugs (anakinra and remdesivir). On the other hand, the cinnamic acid and *o*-hydroxybenzoic acid did not interact in the same regions of reference drugs (Figure 3c).

**Table 1** Values of affinity energy and RMSD from interactions with Mpro enzyme from SARS-CoV-2 (PDB: 6M0K)

| Molecule | Affinity energy (kcal/mol) | RMSD (Å) |
|---|---|---|
| Agathisflavone | -8.3 | 1.603 |
| Amentoflavone | -8 | 1.513 |
| Myricetin-3-O-rhamnoside | -7.6 | 1.759 |
| Quercetin-3-O-rutinoside | -7.4 | 1.231 |
| Quercetin-3-O-rhamnoside | -7.1 | 1.919 |
| Remdesivir* | -6.8 | 1.64 |
| Myricetin | -6.7 | 1.703 |
| Quercetin | -6.7 | 1.941 |
| Anakinra* | -6.5 | 2.058 |
| Azithromycin* | -5.8 | 1.253 |
| Baricitinib* | -5.7 | 1.379 |
| Gallic acid | -5 | 1.471 |
| Protocatechuic acid | -4.9 | 1.716 |
| Ferulic acid | -4.6 | 1.766 |
| p-Coumaric acid | -4.5 | 1.795 |
| p-Hydroxybenzoic acid | -4.5 | 1.395 |
| Cinnamic acid | -3.7 | 1.692 |

*reference drug

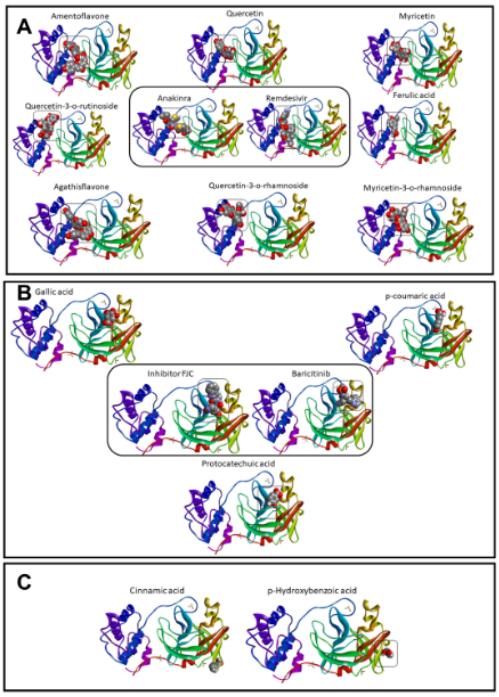


**Figure 3** Sites of interactions by the phytochemicals and control molecules with Mpro from COVID-19 virus, which were organized in group of similar interaction with inhibitor FCJ and Baricitinib (A), Anakinra and Remdesivir (B), and molecules without share of interactions (C).

In the group of inhibitor FJC, as presented in Table 2, all molecules shared interaction with the residue of Glu166A, next to residues of His 164A and Met 165A. The gallic acid presented distances of interactions around 2.0 Å with Glu 166A, like FJC, and *p*-coumaric acid interacted only with this amino acid. The region formed by these residues cited above is essential in the post-transcription process. Besides, the residue of Glu166, and interactions with Ser 144, Gly 143, and Asn142 appear to be related to the binding of inhibitors, being essential to the design of Mpro inhibitors.[35,36] Interactions with residues of Gly 143A, Ser 144A, and Cys 145A, close to Asn 142A residue, were also observed. Interactions with Lys 5A, Lys 137A, and Asp 289A were shared between anakinra and remdesivir, as presented in Table 3. However, agathisflavone, ferulic acid, myricetin, quercetin-3-*O*-rhamnoside, quercetin-3-*O*-rutinoside, and quercetin performed stronger interactions with Asp 289 than anakinra. Besides, interaction with Glu 288A occurred with remdesivir, agathisflavone, ferulic acid, myricetin-3-*O*-rhamnoside, myricetin, quercetin-3-*O*-rhamnoside, and quercetin, but did not occur with anakinra. These same phytochemicals shared with anakinra the interaction with Asp 197A, which did not happen with remdesivir.

**Table 2** Hydrogen bonds interactions between FJC group of molecules and Mpro SARS-CoV-2

| Residue | FJC | GAA | PCA | PRA |
|---|---|---|---|---|
| **Interaction distances (Å)** | | | | |
| His41 | - | - | - | - |
| Gly143 | 2.56 | 2.99 | - | 2.55 |
| Ser144 | 3.45 | 2.11 | - | 2.3 |
| Cys145 | 1.93 | 2.98 | - | 2.7 |
| His164 | 2.36 | - | - | - |
| Met165 | 3.88 | - | - | - |
| Glu166 | 1.83 | 1.99 | 3.63 | 3.65 |
| Pro168 | - | - | - | - |
| Gln189 | 3.03 | - | - | - |

**Table 3** Hydrogen bonds interactions between Anakinra/remdesivir group of molecules and Mpro SARS-CoV-2

| Residue | REM | ANA | AGA | AME | FEA | MOR | MYR | QORh | QORu | Quercetin |
|---|---|---|---|---|---|---|---|---|---|---|
| **Interaction distances (Å)** | | | | | | | | | | |
| Lys5A | 3.23 | 2.67 | 3.22 | 2.67 | 3 | 2.61 | 2.22 | - | - | 2.15 |
| Lys137A | 3.54 | 3.13 | 3.44 | - | - | 3.33 | 3.5 | 3.36 | - | - |
| Asp197A | - | 2.3 | - | - | - | 1.95 | - | 2.36 | 2.96 | - |
| Glu288A | 2.48 | - | 2.65 | - | 1.88 | 2.17 | 3.02 | 2.97 | - | 2.82 |
| Asp289A | 1.86 | 3.42 | 2.06 | - | 1.56 | - | 1.89 | 2.41 | 2.85 | 1.8 |
| Glu290A | - | 2.32 | 2.61 | - | 2.38 | 2.17 | 3.42 | - | - | 2.23 |

## Molecular dynamics

The stability of Mpro-AME and Mpro-AGA complexes were analyzed through the Root Mean Square Deviation (RMSD) and the Root Mean Square Fluctuation (RMSF) present in Figures 2a and 2b, respectively. The Mpro-AME complex (Figure 4a) showed the average RMSD in the value of 2.05 Å, and reached equilibrium from 20 ns simulation, while for the Mpro-AGA complex (Figure 4a) was registered average RMSD of 1.65 Å. This system reached equilibrium from 15 ns of simulation. Therefore, the RMSD results indicated that the Agathisflavone ligand had more stable interactions with the Mpro enzyme than the Amentoflavone molecule. The Mpro-AME complex (Figure 4b) showed a higher fluctuation concerning Mpro-AGA. Therefore, the RMSF results indicated that the binding strength of the Amentoflavone molecule with Mpro enzyme was the weakest, while that the Agathisflavone ligand was the stronger. Besides, the Mpro-AGA complex showed good stability because almost all reside of protein were less than 2.0 Å. The Interaction Potential Energy (IPE) of Mpro-AME and Mpro-AGA complexes are present in Figure 5. This energy was obtained by the sum of Coulomb and Lennard-Jones short-range energies in the last simulation frame (50 ns). The Mpro-AME and Mpro-AGA complexes showed the IPE in the value of -129.630 kJ mol$^{-1}$ and -165.624 kJ mol$^{-1}$, respectively. Therefore, the agathisflavone ligand showed a higher IPE and consequently a higher affinity with the Mpro enzyme than the Amentoflavone.

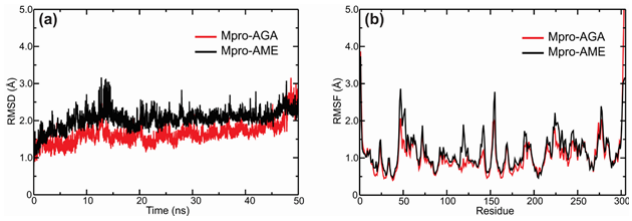


**Figure 4** (a) Root mean square deviation (RMSD), (b) root mean square fluctuation (RMSF) for the Mpro-AME and Mpro-AGA complexes.

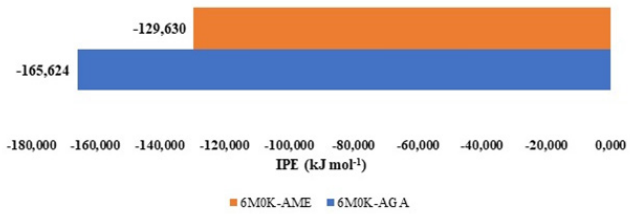


**Figure 5** Interaction Potential Energy (IPE) present in the Mpro-AME and Mpro-AGA complexes.

## Conclusion

The *in silico* studies represent an initial step for the screening of new potential drugs, being evidenced in this work the potential of the

phytochemicals present in the cashew tree against the key enzymes of the replication of SARS-CoV-2, where the biflavonoids amentoflavone and aghatisflavone stand out, these being indicated for future studies *in vitro* and *in vivo*. In this perspective, the present work represents a fundamental step for the development of a pharmacological tool to combat SARS-CoV-2, based on the bioprospecting of natural resources present in the Brazilian northeast.

## Acknowledgments

The authors thank the Fundação Cearense de Apoio ao Desenvolvimento Científico e Tecnológico (Funcap), Coordenação de Aperfeiçoamento de Pessoal de Nível Superior (CAPES) and the Conselho Nacional de Desenvolvimento Científico e Tecnológico (CNPq) for financial support and the scholarship. Alexandre M. Rodrigues Teixeira acknowledges the financial support from the CNPq (Grant#: 305719/2018-1). Hélcio Silva dos Santos acknowledges financial support from the PQ-BPI/FUNCAP (Grant#: BP4-0172-00075.01.00/20). Carla F.C. Fernandes thanks the financial support received from project Inova Fiocruz FUNCAP (Grant#:06481104-2020).

## Conflicts of interest

The authors declare no conflict of interest.

## References

1. VCC Cheng, SKP Lau, PCY Woo, et al. Severe acute respiratory syndrome coronavirus as an agent of emerging and reemerging infection. *Clinical Microbiology Reviews*. 2007;20:694.
2. VM Corman, D Muth, D Niemeyer, et al. Hosts and Sources of Endemic Human Coronaviruses. *Advances in Virus Research*. 2018;100:163–188.
3. N Zhu, D Zhang, W Wang, et al. A Novel Coronavirus from Patients with Pneumonia in China, 2019. *New England Journal of Medicine*. 2020;382(8):727–733.
4. G Li, Y Fan, Y Lai, et al. Coronavirus infections and immune responses. *Journal of Medical Virology*. 2020;92:424–432.
5. MS de CP Brainer, M de F Vidal. Cajucultura nordestina em recuperação. *Caderno Setorial ETENE*. 2018;54:1–13.
6. SK Chabi, H Sina, H Adoukonou-Sagbadja, et al. Antimicrobial activity of Anacardium occidentale L. leaves and barks extracts on pathogenic bacteria. *African Journal of Microbiology Research*. 2014;8:2458–2467.
7. JG da Silva, IA Souza, JS Higino, et al. Antimicrobial activity of the hydroalcoholic extract of Anacardium occidentale Linn. against multi-drug resistant strains of Staphylococcus aureus. *Revista Brasileira de Farmacognosia*. 2017;17:572–577.
8. MSC Oliveira, SM de Morais, DV Magalhães, et al. Antioxidant, larvicidal and anti acetylcholinesterase activities of cashew nut shell liquid constituents. *Acta Tropica*. 2011;117(3):165–170.
9. YS Jaiswal, PA Tatke, SY Gabhe, et al. Antidiabetic activity of extracts of Anacardium occidentale Linn. leaves on n-streptozotocin diabetic rats. *Journal of Traditional and Complementary Medicine*. 2017;7(4):1–14.
10. P Csizmadia. *MarvinSketch and MarvinView: Molecule Applets for the World Wide Web*. 2019;1775.
11. MJS Dewar, EG Zoebisch, EF Healy. Development and use of quantum mechanical molecular models. 76. AM1: a new general purpose quantum mechanical molecular model. *Journal of the American Chemical Society*. 1985.
12. PO Dral, X Wu, L Spörkel, et al. Semiempirical quantum-chemical orthogonalization-corrected methods: theory, implementation, and parameters. *Journal of Chemical Theory and Computation*. 2016;12:1082–1096.
13. JJP Stewart. Optimization of parameters for semiempirical methods VI: More modifications to the NDDO approximations and re-optimization of parameters. *Journal of Molecular Modeling*. 2013;19:1–32.
14. J da Cunha Xavier, FW de Queiroz Almeida-Neto, PT da Silva, et al. Structural characterization, DFT calculations, ADMET studies, antibiotic potentiating activity, evaluation of efflux pump inhibition and molecular docking of chalcone (E)-1-(2-hydroxy-3, 4, 6-trimethoxyphenyl)-3-(4-methoxyphenyl) prop-2-en-1-one. *Journal of Molecular Structure*. 2021;1227:129692.
15. C Milite, G Amendola, A Nocentini, et al. Novel 2-substituted-benzimidazole-6-sulfonamides as carbonic anhydrase inhibitors: synthesis, biological evaluation against isoforms I, II, IX and XII and molecular docking studies. *Journal of Enzyme Inhibition and Medicinal* Chemistry. 2019;34:1697–1710.
16. O Trott, A Olson. Autodock vina: improving the speed and accuracy of docking. *Journal of Computational Chemistry*. 2010;31:455–461.
17. EF Pettersen, TD Goddard, CC Huang, et al. UCSF Chimera - A visualization system for exploratory research and analysis. *Journal of Computational Chemistry*. 2004;25;1605–1612.
18. D Yusuf, AM Davis, GJ Kleywegt, et al. An alternative method for the evaluation of docking performance: RSR vs RMSD. *Journal of Chemical Information and Modeling*. 2008;48:1411–1422.
19. T Gaillard. Evaluation of AutoDock and AutoDock Vina on the CASF-2013 Benchmark. *Journal of Chemical Information and Modeling*. 2018;58:1697–1706.
20. P Borowiecki, AM Wawro, P Wińska, et al. Synthesis of novel chiral TBBt derivatives with hydroxyl moiety. Studies on inhibition of human protein kinase CK2α and cytotoxicity properties. *European Journal of Medicinal Chemistry*. 2004;84:364–374.
21. DS Visualizer. *v4. 0.100. 13345, Accelrys Software Inc*. 2005.
22. D van der Spoel, E Lindahl, B Hess, et al. GROMACS: Fast, flexible, and free. *Journal of Computational Chemistry*. 2005;26:1701–1718.
23. K Lindorff-Larsen, S Piana, K Palmo, et al. Improved side-chain torsion potentials for the Amber ff99SB protein force field, Proteins: Structure. *Function and Bioinformatics*. 2010;78.
24. AW Sousa Da Silva, WF Vranken. ACPYPE - AnteChamber PYthon Parser interface. *BMC Research Notes*. 2012;5:1950–1958.
25. WL Jorgensen, J Chandrasekhar, JD Madura, et al. Comparison of simple potential functions for simulating liquid water. *The Journal of Chemical Physics*. 1983;79:926–935.
26. GB Arfken, HJ Weber, FE Harris. *Mathematical Methods for Physicists, Elsevier.* 2013.
27. GB Arfken, HJ Weber, FE Harris. *Mathematical Preliminaries, in: Mathematical Methods for Physicists*. 2013.
28. G Bussi, D Donadio, M Parrinello. Canonical sampling through velocity rescaling. *Journal of Chemical Physics*. 2007;126:014101.
29. M Parrinello, A Rahman. Polymorphic transitions in single crystals: A new molecular dynamics method. *Journal of Applied Physics*. 1981;52:7182.
30. WF van Gunsteren, HJC Berendsen. A Leap-frog Algorithm for Stochastic Dynamics. *Molecular Simulation*. 1998;1:173–185.
31. W Humphrey, A Dalke, K Schulten. VMD: Visual molecular dynamics. *Journal of Molecular Graphics*. 1996;14:33–38.
32. R Huey, GM Morris, AJ Olson, et al. Software news and update a semiempirical free energy force field with charge-based desolvation. *Journal of Computational Chemistry*. 2017;28:1145–1152.
33. EM Marinho, JB de Andrade Neto, J Silva, et al. Virtual screening based on molecular docking of possible inhibitors of Covid-19 main protease. *Microbial Pathogenesis*. 2020;148:104365.

34. S Das, S Sarmah, S Lyndem, et al. An investigation into the identification of potential inhibitors of SARS-CoV-2 main protease using molecular docking study. *Journal of Biomolecular Structure and Dynamics*. 39(2021)3347–3357.

35. GM Ferreira, T Kronenberger, AK Tonduru, et al. SARS-COV-2 Mpro conformational changes induced by covalently bound ligands. *Journal of Biomolecular Structure and Dynamics*. 2021.

36. ST Ngo, N Quynh Anh Pham, L Thi Le, et al. Computational Determination of Potential Inhibitors of SARS-CoV-2 Main Protease. *Journal of Chemical Information and Modeling*. 2020;60:5771–5780.